CHAPTER 6

PHOTON COUNTING [1) 2) 4) - 12)]

Photon counting is an effective technique used to detect very-low-level-light such as Raman spectroscopy, fluorescence analysis, and chemical or biological luminescence analysis where the absolute magnitude of the light is extremely low. This section describes the principles of photon counting, its operating methods, detection capabilities, and advantages as welll as typical characteristics of photomultiplier tubes designed for photon counting.

6.1 Analog and Digital (Photon Counting) Modes

The methods of processing the output signal of a photomultiplier tube can be broadly divided into analog and digital modes, depending on the incident light intensity and the bandwidth of the output processing circuit.

As Figure 6-1 shows, when light strikes the photocathode of a photomultiplier tube, photoelectrons are emitted. These photoelectrons are multiplied by the cascade process of secondary emission through the dynodes (normally 10^6 to 10^7 times) and finally reach the anode connected to an output processing circuit.

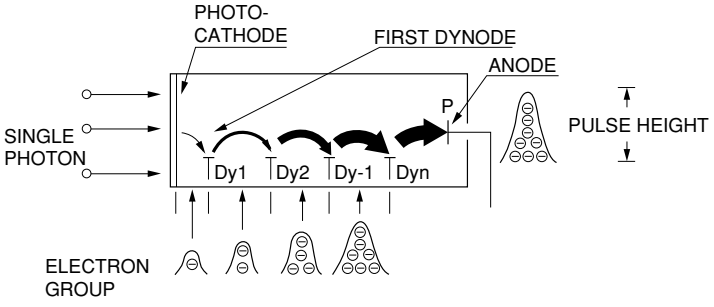

Figure 6-1: Photomultiplier tube operation in photon counting mode

When observing the output signal of a photomultiplier tube with an oscilloscope while varying the incident light level, output pulses like those shown in Figure 6-2 are seen. At higher light levels, the output pulse intervals are narrow so that they overlap each other, producing an analog waveform (similar to (a) and (b) of Figure 6-2). If the light level becomes very low, the ratio of AC component (fluctuation) in the signal increases, and finally the output signal will be discrete pulses (like (c) of Figure 6-2). By discriminating these discrete pulses at a proper binary level, the number of the signal pulses can be counted in a digital mode. This is commonly known as photon counting.

In analog mode measurements, the output signal is the mean value of the signals including the AC components shown in Figure 6-2 (a). In contrast, the photon counting method can detect each pulse shown in Figure 6-2 (c), so the number of counted pulses equals the signal. This photon counting mode uses a pulse height discriminator that separates the signal pulses from the noise pulses, enabling high-precision measurement with a higher signal-to-noise ratio compared to the analog mode and making photon counting exceptionally effective in detecting low level light.

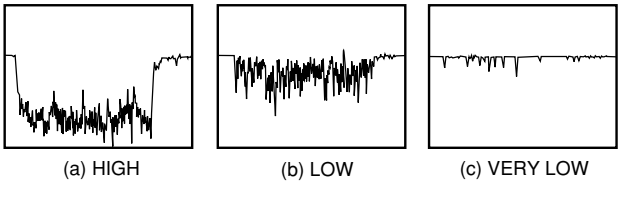

Figure 6-2: Photomultiplier tube output waveforms observed at different light levels

6.2 Principle of Photon Counting

When light incident on a photomultiplier tube becomes very low and reaches a state in which no more than two photoelectrons are emitted within the time resolution (pulse width) of the photomultiplier tube, this light level is called the single photoelectron region and photon counting is performed in this region. Quantum efficiency, an important parameter for photon counting, signifies the probability of photoelectron emission when a single photon strikes the photocathode.

In this single photoelectron region, the number of emitted electrons per photon is one or zero and the quantum efficiency can be viewed as the ratio of the number of photoelectrons emitted from the photocathode to the number of incident photons per unit time. The probability that the photoelectrons emitted from the photocathode (primary electrons) will impinge on the first dynode and contribute to gain is referred to as collection efficiency. Some photoelectrons may not contribute to gain because they deviate from the normal trajectories and are not collected by the first dynode. Additionally, in the photon counting mode, the ratio of the number of counted pulses (output pulses) to the number of incident photons is called detection efficiency or photomultiplier tube counting efficiency and is expressed by the following relation:

$$\text{Detection efficiency (counting efficiency) in the photon counting region} = (Nd/Np) = \eta \times \alpha \quad \cdots \text{(Eq. 6-1)}$$

where Nd is the counted value, Np is the number of incident photons, η is the quantum efficiency of the photocathode and α is the collection efficiency of the dynodes. The detection efficiency greatly depends on the threshold level used for binary processing.

The number of secondary electrons released from the first dynode is not constant. It is around several secondary electrons per primary electron, with a broad probability roughly seen as a Poisson distribution. The average number of electrons per primary electron δ corresponds to the secondary-electron multiplication factor of the dynode. Similarly, this process is repeated through the second and subsequent dynodes until the final electron bunch reaches the anode. In this way the output multiplied in accordance with the number of photoelectrons from the photocathode appears at the anode. If the photomultiplier tube has n stage dynodes, the photoelectrons emitted from the photocathode are multiplied in cascade up to δ^n times and derived as an adequate electron bunch from the anode. In this process, each output pulse obtained at the anode exhibits a certain distribution in pulse height because of fluctuations in the secondary multiplication factor at each dynode (statistical fluctuation due to cascade multiplication), non-uniformity of multiplication depending on the dynode position and electrons deviating from their favorable trajectories. Figure 6-3 illustrates a histogram of photomultiplier tube output pulses. The abscissa indicates the pulse height and the anode output pulses are integrated with time. This graph is known as the pulse height distribution.

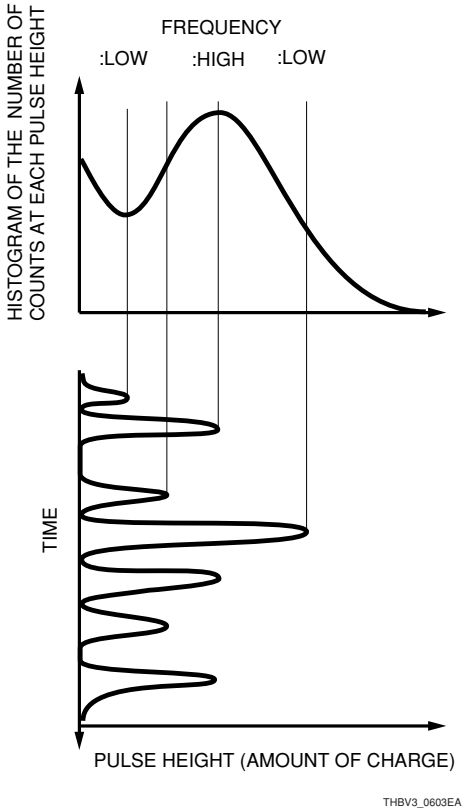

Figure 6-3: Photomultiplier tube output and its pulse height distribution

Figure 6-3 also shows the relation between the pulse height distribution and the actual output pulses obtained with a photomultiplier tube. The pulse height distribu-

tion is usually taken with a multichannel analyzer (MCA) frequently used in scintillation counting applications.

Figure 6-4 (a) shows examples of the pulse height distribution obtained with a photomultiplier tube. There are output pulses present even if no light falls on the photomultiplier tube, and these are called dark current pulses or noise pulses. The broken line indicates the distribution of the dark current pulses, with a tendency to build up somewhat in the lower pulse height region (left side). These dark pulses mainly originate from the thermal electron emission at the photocathode and also at the dynodes. The thermal electrons from the dynodes are multiplied less than those from the photocathode and are therefore distributed in the lower pulse height region.

Figure 6-4 (b) indicates the distribution of the total number of counted pulses S(L) with amplitudes greater than a threshold level L shown in (a). (a) and (b) have differential and integral relations to each other. Item (b) is a typical integral curve taken with a photon counting system using a photomultiplier tube.

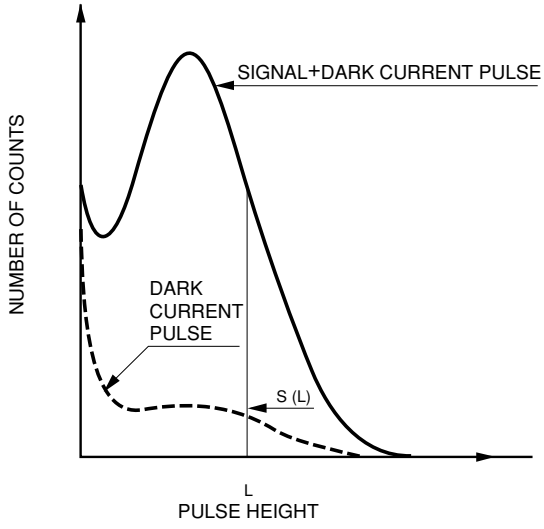

Figure 6-4: Differential and integral representations of pulse height distribution

6.3 Operating Method and Characteristics of Photon Counting

This section discusses specific circuit configurations used to perform photon counting and the basic characteristics involved in photon counting.

(1) Circuit configuration

Figure 6-5 shows a typical circuit configuration for photon counting and a pulse waveform obtained at each circuit.

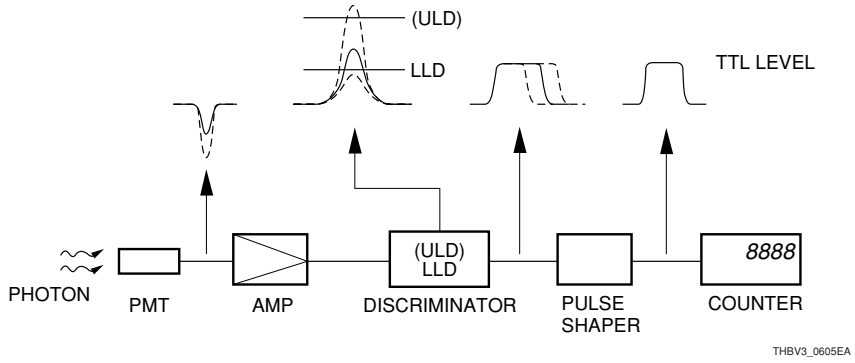

Figure 6-5: Circuit configuration for photon counting

In the above system, current output pulses from a photomultiplier tube are converted to a voltage by a wide-band preamplifier and amplified. These voltage pulse are fed to a discriminator and then to a pulse shaper. Finally the number of pulses is counted by a counter. The discriminator compares the input voltage pulses with the preset reference voltage (threshold level) and eliminates those pulses with amplitudes lower than this value. In general, the LLD (lower level discrimination) level is set at the lower pulse height side. The ULD (upper level discrimination) level may also be often set at the higher pulse height side to eliminate noise pulses with higher amplitudes. The counter is usually equipped with a gate circuit, allowing measurement at different timings and intervals.

(2) Basic characteristics of photon counting

a) Pulse height distribution and plateau characteristics

If a multichannel pulse height analyzer is available, a proper threshold level can be set in the pulse height distribution. Typical pulse height distributions of signal pulses and noise pulses are shown in Figure 6-6. Because the dark current pulses are usually distributed in the lower pulse height region, setting the LLD level in the vicinity of the valley (L_1) of the distribution can effectively eliminate such noise pulses without sacrificing the detection efficiency. In actual operation, however, using a pulse height analyzer is not so popular. Other methods that find plateau characteristics using the circuit of Figure 6-5 are more commonly employed. By counting the total number of pulses with amplitudes higher than the preset threshold level while varying the supply voltage for the photomultiplier tube, plots similar to those shown in Figure 6-7 can be obtained. These plots are called the plateau characteristics. In the plateau range, the change in the number of counts less depends on the supply voltage. This is because only the number of pulses is digitally counted in photon counting, while in the analog mode the gain change of the photomultiplier tube directly affects the change of the output pulse height.

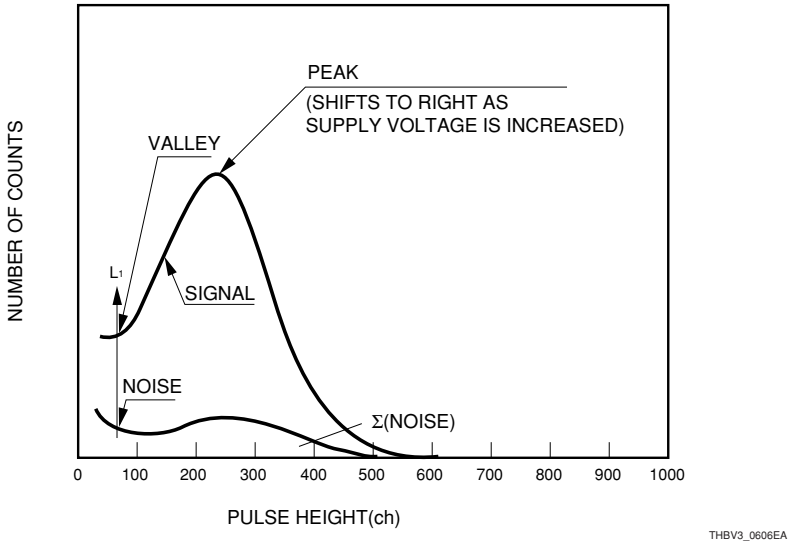

Figure 6-6: Typical example of pulse height distributions

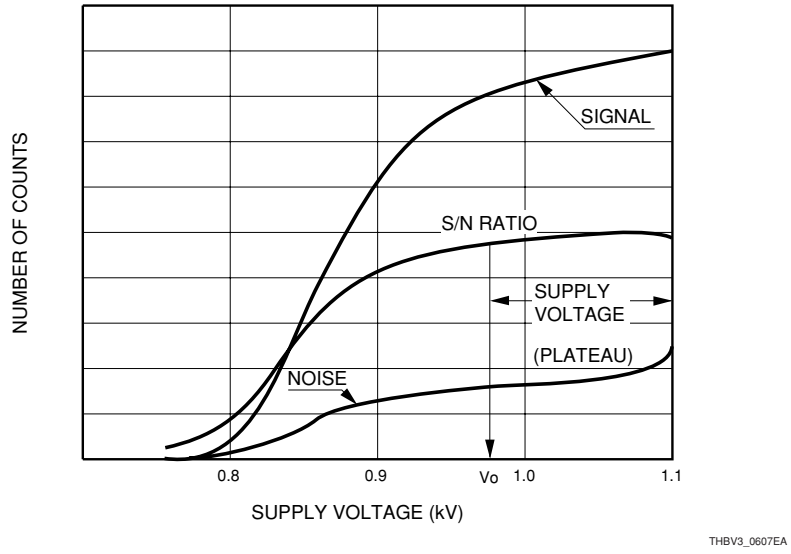

Figure 6-7: Plateau characteristics

b) Setting the photomultiplier tube supply voltage

The signal-to-noise ratio is an important factor from the viewpoint of accurate measurements. Here the signal-to-noise ratio is defined as the ratio of the mean value of the signal count rate to the fluctuation of the counted signal and noise pulses (expressed in standard deviation or root mean square). The signal-to-noise ratio curve shown in Figure 6-7 is plotted by varying the supply voltage, the same procedure which is used to obtain the plateau characteristics. This figure implies that the photomultiplier tube should be operated in the range between the voltage (Vo) at which the plateau region begins and the maximum supply voltage.

c) Count rate linearity

The photon counting mode offers excellent linearity over a wide range. The lower limit of the count rate linearity is determined by the number of dark current pulses, and the upper limit by the maximum count rate. The maximum count rate further depends on pulse-pair resolution, which is the minimum time interval at which each pulse can be separated. The reciprocal of this pulse pair resolution would be the maximum count rate. However, since most events in the photon counting region usually occur at random, the counted pulses may possibly overlap. Considering this probability of pulse overlapping (count error caused by pulse overlapping), the actual maximum count rate will be about one-tenth of the calculated above. Here, if we let the true count rate be N (s^{-1}), measured count rate be M (s^{-1}) and time resolution be t (s^{-1}), the loss of count rate N - M can also be expressed using the dead time M·t caused by pulse overlapping, as follows:

$N - M = N \cdot M \cdot t$

The true count rate N then becomes

$$N = \frac{M}{1 - M \cdot t} \quad \text{(Eq. 6-2)}$$

The count error can be corrected by using this relation.

Figure 6-8 shows examples of count rate linearity data before and after correction, measured using a system with a pulse pair resolution of 18 nanoseconds. The count error is corrected to within 1 % even at a count rate exceeding 10^7 s^{-1}.

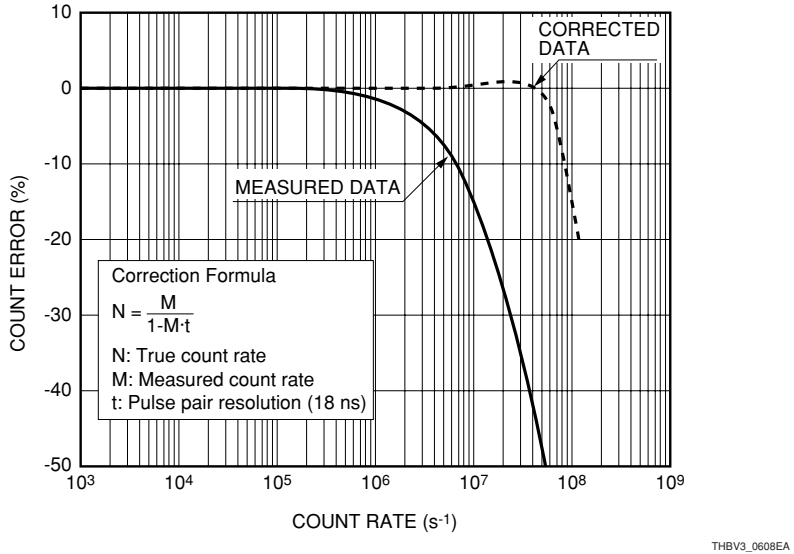

Figure 6-8: Linearity of count rate

d) Advantages of photon counting

Photon counting has many advantages in comparison with the analog mode. Among them, stability and signal-to-noise ratio are discussed in this section.

(I) Stability

One of the significant advantages photon counting offers is operating stability. The photon counting mode is resistant to variations in supply voltage and photomultiplier tube gain. If the supply voltage is set within the plateau region, a change in the voltage has less effect on the output counts. In the analog mode, however, it affects the output current considerably. Immunity to variations in the supply voltage means that the photon counting mode also assures high stability against gain fluctuation of the photomultiplier tube. Normally the photon counting mode offers several times higher immunity to such variations than the analog mode. (Refer to Figure 6-9.)

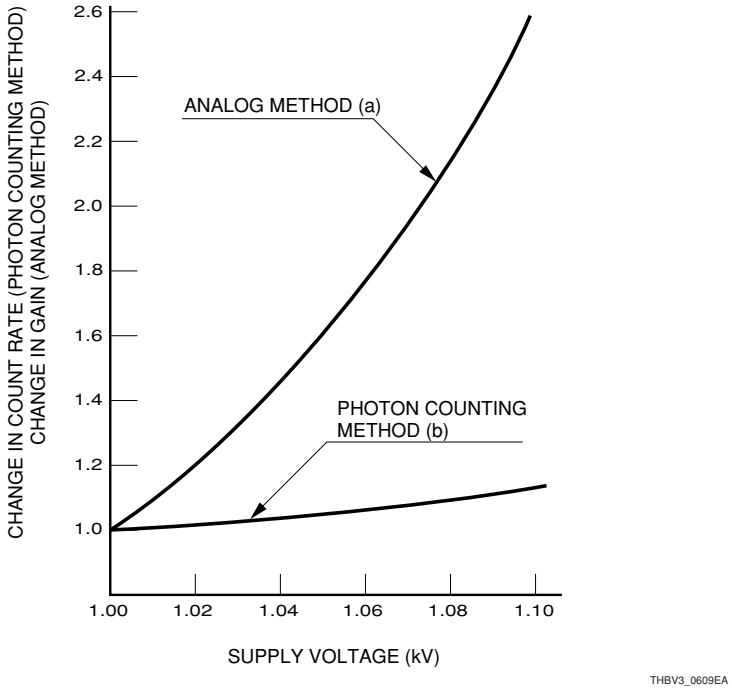

Figure 6-9: Stability versus changes in supply voltage

(II) Signal-to-noise ratio

When signal light strikes the photocathode of a photomultiplier tube, photoelectrons are emitted and directed to the dynode section where secondary electrons are produced. The number of photoelectrons produced per unit time and also the number of secondary electrons produced are determined by statistical probability of events which is represented by a Poisson distribution. The signal-to-noise ratio is also described in 4.3.7 in Chapter 4. The AC component noise which is superimposed on the signal can be categorized by origin as follows

(1) Shot Noise resulting from signal light
(2) Shot Noise resulting from background light
(3) Shot Noise resulting from dark current

In the analog mode, the signal-to-noise ratio[2) - 9, 11)] of the photomultiplier tube output including these shot noises becomes

$$\text{SN ratio(current)} = \frac{Iph}{\sqrt{2eNFB\{Iph+2(Ib+Id)\}}} \quad \cdots\cdots \text{(Eq. 6-3)}$$

where

Iph: signal current produced by incident light (A)
e: electron charge (c)
NF: noise figure of the photomultiplier tube
Ib: cathode current resulting from background light (A)
Id: cathode current resulting from dark current (A)
B: Bandwidth of measurement system (Hz)

Here the true signal current Iph is obtained by subtracting Ib+Id from the total current. The noise originating from the latter-stage amplifier is considered to be negligible because the typical gain μ of a photomultiplier tube is sufficiently large.

The signal-to-noise ratio in the photon counting mode is given by the following equation.

$$\text{SN ratio} = \frac{Ns\sqrt{T}}{\sqrt{Ns+2(Nb+Nd)}} \quad \cdots\cdots \text{(Eq. 6-4)}$$

where

Ns: number of counts/sec resulting from incident light per second
Nb: number of counts/sec resulting from background light per second
Nd: number of counts/sec resulting from dark current per second
T: measurement time (s)

Here the number of counts/sec of true signals Ns is obtained by subtracting Nb+Nd from the total number of counts.

From the common equivalent relation between the time and frequency (T=1/2B), if B=1 (Hz) and T=0.5 (s), then the signal-to-noise ratio will be as follows:

in the analog mode

$$\text{SN ratio(current)} = \frac{Iph}{\sqrt{2eNFB\{Iph+2(Ib+Id)\}}} \quad \cdots\cdots \text{(Eq. 6-5)}$$

in the photon counting mode

$$\text{SN ratio} = \frac{Ns}{\sqrt{2\{Ns+2(Nb+Nd)\}}} \quad \cdots\cdots \text{(Eq. 6-6)}$$

Through the above analysis, it is understood that the photon counting mode provides a better signal-to-noise ratio by a factor of the noise figure NF. Since the dark current includes thermal electrons emitted from the dynodes in addition to those from the photocathode, its pulse height distribution will be shifted toward the lower pulse height side. Therefore, the dark current component can be effectively eliminated by use of a pulse height discriminator while maintaining the signal component, assuring further improvement in the signal-to-noise ratio. In addition, because only AC pulses are counted, the photon counting mode is not influenced by the DC leakage current. Amplifier noises can totally be eliminated by a discriminator.

References in Chapter 6

1) IEC PUBLICATION 306-4, 1971.
2) Illes P. Csorba "Image Tubes" Howard W, Sams & Co. (1985).
3) F. Robben: Noise in the Measurement of Light with PMs, pp. 776-, Appl. Opt., 10, 4 (1971).
4) R. Foord, R. Jones, C. J. Oliver and E. R. Pike: Appl. Opt., 8, 10, (1969).
5 R. Foord, R. Jones, C.J. Oliver and E.R. Pike: Appl. Opt. 1975, 8 (1969).
6) J.K. Nakamura and S.E. Schmarz: Appl. Opt., 1073, 7, 6 (1968).
7) J.K. Nakamura and S. E. Schwarz: Appl. Opt., 7, 6 (1968).
8) R.R. Alfano and N. Ockman: Journal of the Optical Society of America, 58, 1 (1968).
9) T. Yoshimura, K. Hara and N. Wakabayashi: Appl. Optics, 18, 23 (1979).
10) T.S. Durrani and C. A. Greated: Appl. Optics, 14, 3 (1975).
11) Hamamatsu Photonics Technical Publication: Photon Counting (2001).
12) A. Kamiya, K. Nakamura, M. Niigaki: Journal of the Spectropscopical Society of Japan, 52, 4, 249 (2003).